

## **DAMAGE IDENTIFICATION OF BRIDGE CRANE METAL STRUCTURE BASED ON MODE SHAPE CURVATURE AND RSM**

Yifei TONG<sup>1</sup>, Meng ZHONG<sup>1</sup>, Xu ZHANG<sup>2</sup>, Xiangdong LI<sup>3\*</sup>

*In order to maintain the integrity and safety of crane metal structure, a damage identification method based on mode shape curvature and response surface methodology (RSM) is proposed in this paper. Basically, mode curvature method is used to identify damage location. Then the central composite design method is selected to establish quadratic response surface for identification of damage severity. Finally, numerical simulation of a QD50/10-31.5A5 universal bridge crane is conducted to verify the proposed method. The results show that the proposed method can identify multiple damage of the structure accurately with improved identification efficiency due to the application of RSM.*

**Keywords:** Crane metal structure, Mode shape curvature, Response surface methodology, Finite element analysis, Damage identification.

### **1. Introduction**

Scientific evaluation of health condition for crane metal structure is of critical importance in security precaution and maintenance [1]. Damage identification as a basis of structural health monitoring is drawing a significant amount of research attentions. At present, damage identification method can be divided into two categories. One is local damage identification based on the non-destructive testing and sensor technology, and the other is global damage identification based on static or dynamic parameters of structures [2]. The method of using structural dynamic parameters has great theoretical study value and wide application prospect due to high efficiency and low cost [3]. Lu et al. studied the sensitivity of general dynamic response of a structure with respect to a perturbation of a system parameter and proposed a damage identification method based on dynamic response sensitivity, which could detect the damage of steel beams accurately [4]. Diao et al. proposed a damage identification method based on transmissibility function and support vector machine, and an offshore platform

<sup>1</sup> Nanjing University of Science and Technology, China

<sup>2</sup> AECC SOUTH INDUSTRY CO., LTD, China

<sup>3</sup> Jiangsu Province Special Equipment Safety Supervision Inspection Institute, China, e-mail: tyf51129@aliyun.com

under white noise excitation were conducted to verify the proposed method [5]. Cha et al. used modal strain energy as damage index to identify the damage severity of a 3D frame structure based on hybrid multi-objective optimization [6]. The above literatures show that the methods of damage identification based on structural dynamic response are mostly used for structures such as beams and small-sized welded frames, and there are few studies on crane metal structure.

The response surface methodology (RSM) is actually a combination of statistical and mathematical theory, firstly proposed by Box and Wilson for operation conditions optimization in the chemical industry [7]. In recent years, researchers have found the application value of RSM in the field of damage identification. Umar et al. presented an alternative model updating method for damage detection based on RSM using frequencies and mode shapes [8]. Mukhopadhyay et al. carried out a comparative assessment of the damage identification capability of five DOE methods used in RSM, and revealed that central composite design and D-optimal design are most recommendable for structural damage identification [9]. However, the application of RSM is currently limited to the damage localization, and it is necessary to extend RSM to the damage severity identification of structures.

Considering the importance of the evaluation of crane metal structure, mode shape curvature and RSM are combined to perform the damage identification of location and severity. Taking bridge crane as an example, the change rate of first two mode shape curvature before and after the damage is selected as damage index to determine damage location. On the basis of damage localization, the central composite design is applied to establish quadratic response surface model to predict the damage severity of damaged location.

## 2. Damage location identification based on mode shape curvature

### 2.1. Mode shape curvature

Compared with natural frequency which simply indicates the overall characteristics of the structure, mode shape curvature (MSC) not only contains position information of the structure but also is more sensitive to local damage, and is widely used for damage identification of civil and mechanical engineering structures. Crane metal structure is a kind of large-span welded box beam, which is mainly subjected to vertical load and bending deflection. For Euler-Bernoulli beam in elastic range, the curvature can be calculated by expression:

$$\rho = \frac{M}{EI} \quad (1)$$

where  $\rho$  is the bending curvature of the beam,  $M$  and  $EI$  are the bending moment and rigidity of the beam section, respectively.

According to modal analysis theory, vibration displacement is approximate to:

$$u(x, t) = \sum_{i=1}^N \phi_i(x) q_i(t) \quad (2)$$

where  $u(x, t)$  denotes the vibration displacement of section  $x$  at time  $t$ ,  $\phi_i(x)$  and  $q_i(t)$  are the mode shapes and modal coordinates respectively,  $N$  denotes the total number of modes to be considered.

For elastic beams, curvature is defined by the second derivative of vibration displacement:

$$v(x) = \frac{\partial^2 u(x, t)}{\partial x^2} = \sum_{i=1}^N \phi_i''(x) q_i(t) \quad (3)$$

where  $v(x)$  is the MSC.

According to Eqs. (1), (2) and (3), when the crane metal structure has defects such as weld cracks, material properties degradation and corrosion, the elastic modulus and bending rigidity of the corresponding damage position will be decreased, and the MSC at damage location will be increased. As a result, damage location can be identified by utilizing the rate of change of MSC before and after the damage.

## 2.2. Damage index

In the process of damage localization, the MSC can be obtained by the experimentally measured or numerically calculated mode shapes using the central difference approximation [10]:

$$v_{ik} = \frac{\phi_{(i-1)k} - 2\phi_{ik} + \phi_{(i+1)k}}{l_{(i-1,i)} \cdot l_{(i,i+1)}} \quad (4)$$

where  $v_{ik}$  is the MSC,  $\phi_{ik}$  is the displacement of mode  $k$  at node  $i$ ,  $i$  and  $k$  denote the node and mode number respectively,  $l_{(i-1,i)}$  and  $l_{(i,i+1)}$  denote the distance between node  $i$  and its adjacent nodes.

Damage index is defined by:

$$DI_{ik} = \frac{v_{ik}^d - v_{ik}^u}{v_{ik}^u} \quad (5)$$

where  $v_{ik}^u$  and  $v_{ik}^d$  represent the MSC of crane metal structure in undamaged and damaged states separately.

The  $k$ th mode damage indices are arranged as a damage vector by node number:

$$DIVv_k = [DI_{1k}, DI_{2k}, \dots, DI_{ik}, \dots, DI_{lk}]^T \quad (6)$$

The locations can be detected by using the damage index  $DI_{ik}$  and vector  $DIVv_k$ . It is worth mentioning that when the  $k$ th MSC at node  $i$  is close to zero ( $v_{ik}^u \approx 0$ ), the damage index  $DI_{ik}$  will be abrupt even if no damage occurs according to Eq. (5). The node with  $v_{ik}^u \approx 0$  is defined as the zero point of curvatures, obviously, it will cause errors in the process of damage localization. In order to eliminate the errors caused by the zero point of curvatures effectively, the processing method is as follows:

If  $\frac{|v_{jk}^u|}{\max_k |v_{jk}^u|} \leq 0.1$ , the node  $j$  can be considered as a zero point of curvatures, and the corresponding damage factor is calculated according to the following formula:

$$DI_{jk} = \frac{v_{jk}^d - v_{jk}^u}{\sqrt{v_{jk}^u \cdot \max_k |v_{jk}^u|}} \quad (7)$$

Finally, damage index calculation formula is obtained by combining Eqs. (5) and (7):

$$DI_{ik} = \begin{cases} \frac{v_{ik}^d - v_{ik}^u}{v_{ik}^u}, & \frac{|v_{ik}^u|}{\max_k |v_{ik}^u|} > 0.1 \\ \frac{v_{ik}^d - v_{ik}^u}{\sqrt{|v_{ik}^u| \cdot \max_k |v_{ik}^u|}}, & \frac{|v_{ik}^u|}{\max_k |v_{ik}^u|} \leq 0.1 \end{cases} \quad (8)$$

### 2.3. The process of damage localization

The general damage localization process of crane metal structure based on MSC is as follows: Compute the mode shape curvatures from experimentally measured or numerically calculated mode shapes firstly; Then obtain the damage index according to Eqs. (4) and (8); Ultimately, using the vector shown in Eq. (6) detect the damage location. Fig. 1 depicts a schematic diagram of the proposed damage location identification.

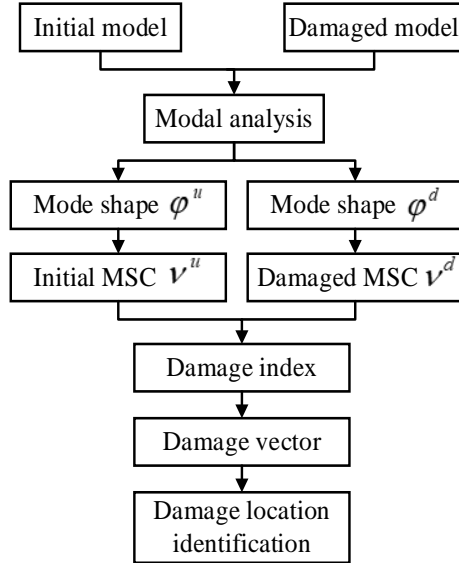


Fig. 1. Schematic diagram of damage location identification based on MSC

### 3. Damage severity detection based on RSM

#### 3.1. Response surface methodology

The essence of RSM is to represent the response  $y$  of a physical structure by the input parameter  $x$  through a mathematical model:

$$y = f(x_1, x_2, \dots, x_k) + \delta \quad (9)$$

where  $f(\cdot)$  is the mapping function,  $\delta$  is the variability factor not considered in function  $f(\cdot)$ ,  $k$  denotes the number of input parameters. In this paper, the quadratic response surface model with high fitting precision is used to identify the damage severity, and the function is expressed as:

$$y = f(x_1, x_2, \dots, x_k) + \delta = \beta_0 + \sum_{i=1}^k \beta_i x_i + \sum_{i=1}^k \beta_{ii} x_i^2 + \sum_{i < j, j=2}^k \beta_{ij} x_i x_j + \delta \quad (10)$$

where  $\beta_0$ ,  $\beta_i$ ,  $\beta_{ii}$  and  $\beta_{ij}$  are the constant, primary, quadratic and cross term coefficients of response surface model, respectively [11].

#### 3.2. The process of damage severity detection

Based on the results of localization, the established response surface model is used to identify the damage severity. In order to quantify the damage, the

damage of crack is equivalent to the reduction of Young modulus at the corresponding damage position:

$$d_x = \frac{E_x^u - E_x^d}{E_x^u} \cdot 100\% \quad (11)$$

where  $x$  is the damage position coordinate,  $d_x$  is the damage severity,  $E_x^u$  and  $E_x^d$  are the elastic modulus before and after the damage, respectively.

The process of identifying the multiple damage severity of crane metal structure based on RSM is as follows:

Step 1. Select appropriate experimental design method and combine the analysis software Design-Expert [12] to establish the response surface model between damage severity and damage index:

$$DI_{ik} = f_{ik}(d_1, d_2 \dots d_x) \quad (12)$$

where  $DI_{ik}$  is the  $k$ th mode damage index at node  $i$ ,  $f_{ik}(\cdot)$  is the function quadratic response surface model.

Step 2. Establish an optimization model with minimum the residual between response surface model and actual damage index according to the damage test sample  $(d_i^t, DI_{ik}^t)$ . The optimization model is as follows:

$$\begin{aligned} \min \sum_{i=1}^x \left\| f_{ik}(d_1, d_2 \dots d_x) - DI_{ik}^t \right\|^2 \\ \text{s.t. } d_1, d_2 \dots d_x \in [0, 50] \end{aligned} \quad (13)$$

Step3. Compute the optimization model in Eq. (13) using Matlab, and compare the result  $(d_1, d_2, \dots, d_m)$  with the test sample damage  $(d_1^t, d_2^t, \dots, d_m^t)$  to verify the accuracy of the proposed method.

## 4. Numerical study

### 4.1. Bridge crane metal structure

The metal structure of universal bridge crane (QD50/10-31.5A5) consists of main girder and end beam, as shown in Fig. 2. The main girder with a span of 31500 mm is welded by upper and lower flange plates and two webs, of which 57 diaphragms are used as supporting structure. The end beam is also welded by flange plates and webs, with a span of 5900 mm and seven large diaphragms inside as supporting structure.

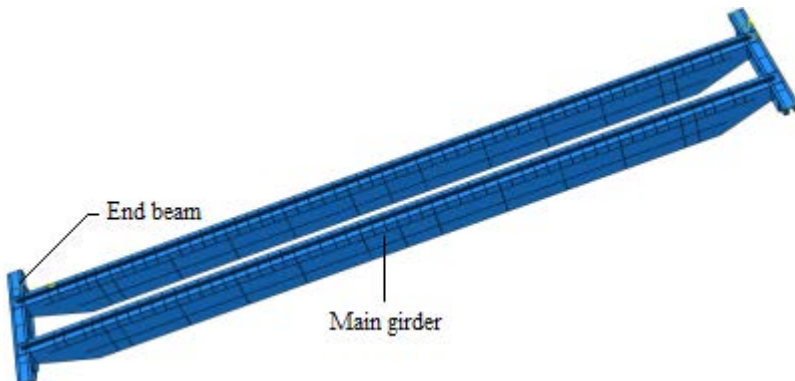
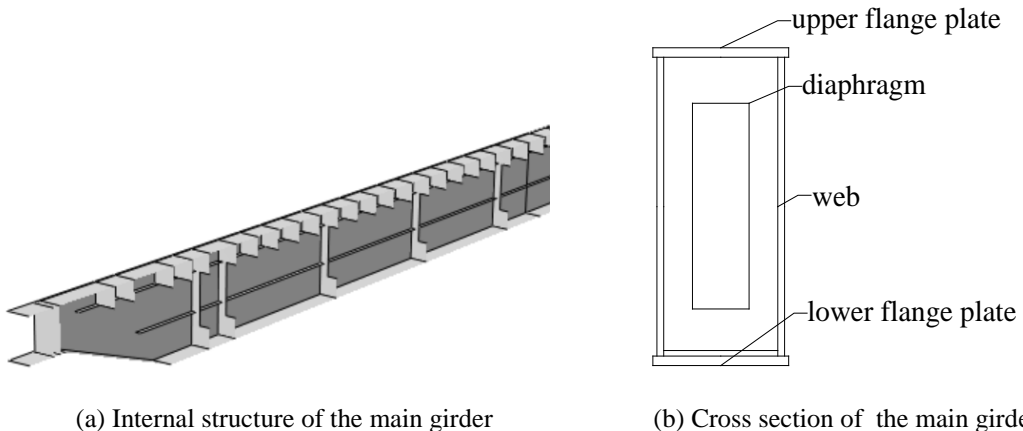


Fig. 2. Bridge crane metal structure

When the crane is working, the metal structure is mainly subjected to vertical loads. The lower flange plate of main girder is under tensile stress due to bending deformation, and the welding area between the plate and webs is the hot spots of stress and damages. Therefore, the problem of crane metal structure damage identification can be simplified to the damage identification of the main girder. The numerical model of main girder is established using the finite element software ABAQUS, and the type of element is S4R(a 4-node doubly curved thin or thick shell, reduced integration). The internal structure and cross section of the main girder are shown in Fig. 3.



(a) Internal structure of the main girder (b) Cross section of the main girder  
Fig. 3. Main girder structure

Considering that damages generally occur at the welding area between the lower flange plate and webs, 130 nodes on the center line of lower flange plate are selected as modal displacement output points, and 129 localization elements are constructed, as shown in Fig. 4. The damage location can be identified by changes in MSC of the selected nodes.

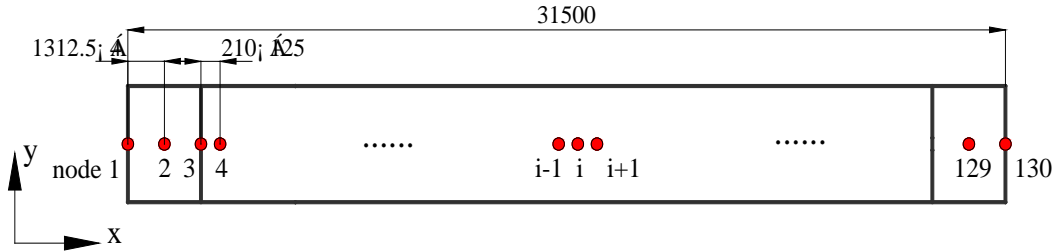


Fig. 4. Schematic diagram of modal displacement output nodes

#### 4.2. Damage condition

In the process of localization, structural damage can be simulated by cutting cracks at the welding area between the main girder lower flange plate and webs. The dimension of cracks is  $140\text{mm} \times 30\text{mm}$ , and one single damage and two multiple damage cases are analyzed in this paper.

Case one (single damage): Crack occurs at the weld of lower flange plate and webs at element 65.

Case two (multiple damage): Cracks occur at the weld of lower flange plate and webs at elements 33 and 65.

Case three (multiple damage): Cracks occur at the weld of lower flange plate and webs at elements 33, 65 and 97.

#### 4.3. Damage location identification

The modal analyses of the main girder in healthy and damaged states are performed using ABAQUS, and the mode shapes of the 130 nodes in the center line of lower flange plate is extracted as the characteristics of the 129 elements. Then, the MSC of each node is calculated by Eq. (4), and the damage index is calculated by Eq. (5). Finally, damage locations are determined according to the damage vector  $DIVv_k$  (Eq. 6). The results of damage locations identification using the first two mode shape curvatures of main girder are shown in Fig. 5 to Fig 7.

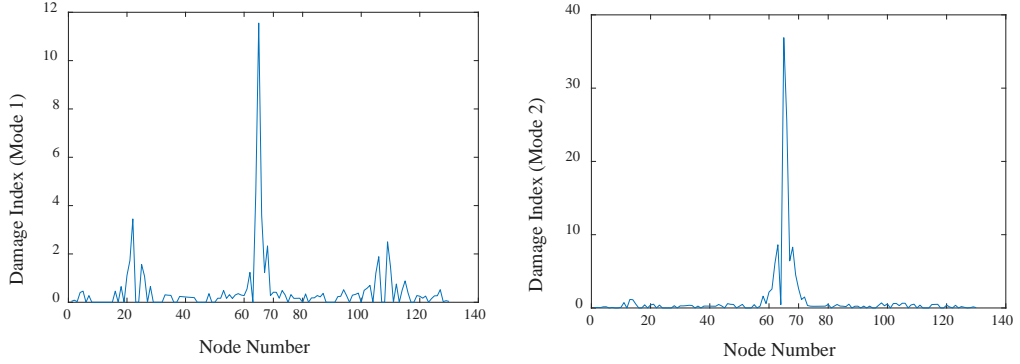


Fig. 5. Damage location identification of case one

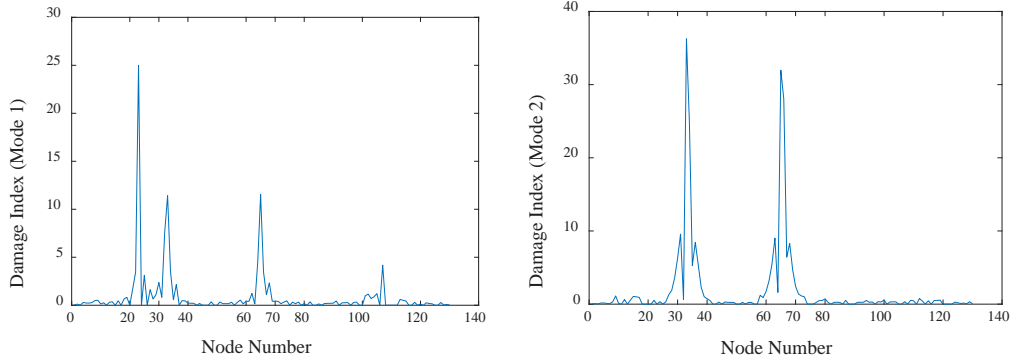


Fig. 6. Damage location identification of case two

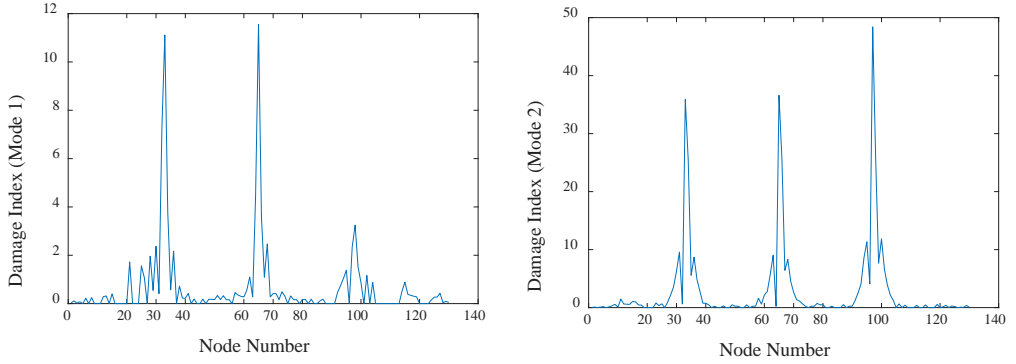


Fig. 7. Damage location identification of case three

The damages of the three cases are detected by using second mode shape curvatures, while the first mode shape curvatures have errors in case two due to the existence of curvature zero point at node 23. The curvature zero point is processed using Eq. (8), and the optimization result of case two is shown in Fig. 8.

In summary, multiple damage of the crane metal structure can be determined based on MSC exactly, and the identification accuracy of the second mode shape curvature is higher than the first.

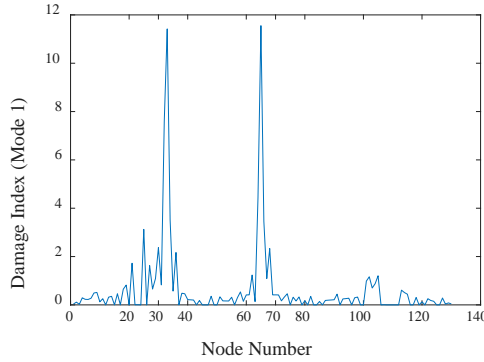


Fig. 8. Optimization result of case two based on first mode shape curvature

#### 4.4. Damage severity identification

Taking case three as an example, the feasibility of multiple damage severity identification based on RSM is studied. Unlike the localization of damage, quantification of damage is required to damage severity identification. Therefore, the cracks in damage cases should be equivalent to the decrease of Young modulus. Composite central design (CCD) is selected to establish a response surface model between damage severity and second mode damage index. The damage indices of elements 33, 65 and 97 are defined as  $DI_{33}$ ,  $DI_{65}$  and  $DI_{97}$  according to Eq. (8), and the damage severity of nodes 33, 65 and 97 are defined as  $d_{33}$ ,  $d_{65}$  and  $d_{97}$  according to Eq. (11). The samples based on CCD are shown in Table 1. Quadratic response surface functions are obtained by fitting the sample data, as shown in Eqs. (14) to (16).

Table 1  
Numerical experimental samples of case three based on CCD

| Sample number | damage severity / % |          |          | Second mode damage index / % |           |           |
|---------------|---------------------|----------|----------|------------------------------|-----------|-----------|
|               | $d_{33}$            | $d_{65}$ | $d_{97}$ | $DI_{33}$                    | $DI_{65}$ | $DI_{97}$ |
| 1             | 5                   | 5        | 5        | 4.40                         | 4.64      | 3.91      |
| 2             | 45                  | 5        | 5        | 71.43                        | 1.64      | 3.91      |
| 3             | 5                   | 45       | 5        | 4.03                         | 56.01     | 3.56      |
| 4             | 45                  | 45       | 5        | 69.96                        | 52.73     | 3.20      |
| 5             | 5                   | 5        | 45       | 4.03                         | 1.91      | 51.96     |
| 6             | 45                  | 5        | 45       | 70.33                        | -1.09     | 51.25     |
| 7             | 5                   | 45       | 45       | 2.93                         | 58.20     | 49.82     |

|    |       |       |       |        |       |       |
|----|-------|-------|-------|--------|-------|-------|
| 8  | 45    | 45    | 45    | 69.23  | 55.19 | 49.47 |
| 9  | 8.64  | 25    | 25    | 7.33   | 21.86 | 22.42 |
| 10 | 58.64 | 25    | 25    | 117.95 | 23.50 | 21.35 |
| 11 | 25    | 8.64  | 25    | 29.67  | 10.11 | 22.78 |
| 12 | 25    | 58.64 | 25    | 27.11  | 93.17 | 20.28 |
| 13 | 25    | 25    | 8.64  | 29.30  | 24.59 | 6.05  |
| 14 | 25    | 25    | 58.64 | 27.84  | 19.13 | 84.34 |
| 15 | 25    | 25    | 25    | 28.94  | 23.22 | 22.06 |

$$\begin{aligned}
 DI_{33} = f_1(d_{33}, d_{65}, d_{97}) = & -0.51 + 0.61d_{33} + 0.03d_{65} + 0.02d_{97} \\
 & - 3.44 \cdot 10^{-4} d_{33}d_{65} - 1.13 \cdot 10^{-4} d_{33}d_{97} - 1.13 \cdot 10^{-4} d_{65}d_{97} \quad (14) \\
 & + 0.02d_{33}^2 - 9.59 \cdot 10^{-4} d_{65}^2 - 7.99 \cdot 10^{-4} d_{97}^2
 \end{aligned}$$

$$\begin{aligned}
 DI_{65} = f_2(d_{33}, d_{65}, d_{97}) = & 0.11 - 1.17 \cdot 10^{-3} d_{33} + 0.55d_{65} - 0.05d_{97} \\
 & - 9.06 \cdot 10^{-5} d_{33}d_{65} + 8.44 \cdot 10^{-5} d_{33}d_{97} + 3.16 \cdot 10^{-3} d_{65}d_{97} \quad (15) \\
 & - 6.71 \cdot 10^{-4} d_{33}^2 + 0.02d_{65}^2 - 1.4 \cdot 10^{-3} d_{97}^2
 \end{aligned}$$

$$\begin{aligned}
 DI_{97} = f_3(d_{33}, d_{65}, d_{97}) = & -0.25 + 0.02d_{33} + 0.03d_{65} + 0.54d_{97} \\
 & - 7.65 \cdot 10^{-18} d_{33}d_{65} - 2.19 \cdot 10^{-4} d_{33}d_{97} - 8.94 \cdot 10^{-4} d_{65}d_{97} \quad (16) \\
 & - 5.33 \cdot 10^{-4} d_{33}^2 - 8.46 \cdot 10^{-4} d_{65}^2 + 0.01d_{97}^2
 \end{aligned}$$

Three groups of the damage test samples and the second mode damage index are obtained by combining different damage severity values, as shown in Table 2. An optimization model of damage severity identification is established by substituting the second mode shape curvature damage index ( $DI_{33}^t, DI_{65}^t, DI_{97}^t$ ) of the test sample and the response surface functions ( $f_1, f_2, f_3$ ) into Eq. (13). The global optimal algorithm GlobalSearch is used to solve the optimization model, and the results of damage severity identification are shown in Figs. 9 to 11.

Table 2  
Damage test samples

| Test sample | Element | damage severity / % | Second mode damage index / % |
|-------------|---------|---------------------|------------------------------|
| Group one   | 33      | 12                  | 12.1                         |
|             | 65      | 14                  | 13.1                         |
|             | 97      | 16                  | 13.2                         |
| Group two   | 33      | 10                  | 9.2                          |
|             | 65      | 20                  | 18.9                         |
|             | 97      | 30                  | 28.1                         |
| Group three | 33      | 20                  | 21.2                         |
|             | 65      | 30                  | 26.2                         |
|             | 97      | 40                  | 42.0                         |

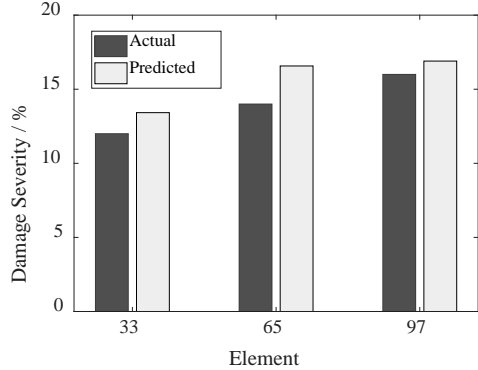


Fig. 9. Results of group one

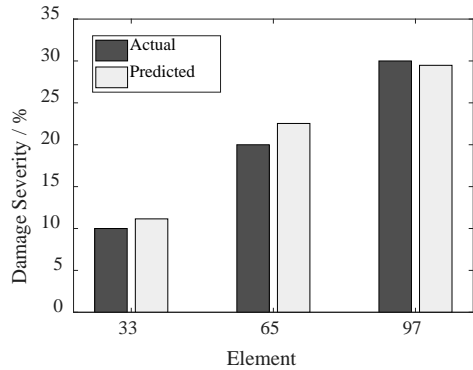


Fig. 10. Results of group two

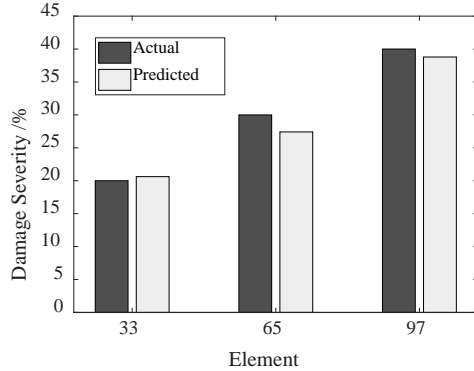


Fig. 11. Results of group three

From the predicted results of Figs. 9 to 11. Multiple damage severity of the structure can be determined using RSM, and the lowest and highest recognition accuracy are 84.5% and 98.3% respectively. Moreover, when the damage severity values of elements 33, 65 and 97 are relatively dispersed (corresponding to the test samples of group two and three), the accuracy of identification is above 90%. Conversely, the accuracy is lower when the values of damage severity are more concentrated (corresponding to group one). In general, the multi-damage severity identification of crane metal structure based on RSM has convincing precision, and the number of experimental samples is reduced compared with intelligent algorithms such as artificial neural network [13] and support vector machine [14], which improves the efficiency of multi-damage identification.

## 5. Conclusions

A damage identification method based on MSC and RSM is proposed to detect the multiple damage of a crane metal structure in this paper. The main girder of crane is divided into 129 elements, and the MSC change rate of each element before and after the damage is defined as the damage index for localization. On the basis of localization, the quadratic response surface model between second mode damage index and damage severity based on CCD is used to identify damage severity. The results indicate:

(1) The MSC is more sensitive to local damage of crane metal structure than natural frequency. The first two mode shape curvatures can be used to identify the local crack with a size of  $140mm \times 30mm$ , and the damage identification effect of the second mode shape curvature is better than the first.

(2) The average error of damage severity detection using the proposed method is  $7.7\% < 10\%$ , which meets the general accuracy requirements. Moreover, compared with the method based on artificial neural network or support vector machine, The RSM only needs 15 samples to identify the severity of damages at three different locations of the structure, and the amount of experimental samples are reduced effectively, which improves the efficiency of damage detection of crane metal structure and other similar large mechanical structures.

## Acknowledgments

This work was financially supported by the Program of Science Foundation of General Administration of Quality Supervision and Inspection of Jiangsu Province (KJ175940). The supports are gratefully acknowledged.

Conflicts of Interest: The authors declare no conflict of interest.

## R E F E R E N C E S

- [1]. *N. Y. Qing, Y. X. Xia, X. W, Ye*, “Structural health monitoring of a tall building with huge floating platform”, in Advances in Science and Technology, 2013, pp. 177-187.
- [2]. *A. Katunin, K. Dragan*, “Damage identification in aircraft composite structures: A case study using various non-destructive testing techniques”, in Composite structures, Vol. 127, 2015, pp. 1-9.
- [3]. *W. D. Scott, R. F. Charles, B. P. Michael*, “A summary review of vibration-based damage identification methods”, in Shock and vibration digest, Vol. 30, no. 2, 1998, pp. 91-105.
- [4]. *Z. R. Lu, S. S. Law*, “Features of dynamic response sensitivity and its application in damage detection”, in Journal of sound and vibration, Vol. 303, no. 1-2, 2007, pp. 305-329.
- [5]. *Y. Diao, X. Men, Z. Sun, K. Guo, Y. Wang*, “Structural Damage Identification Based on the Transmissibility Function and Support Vector Machine”, in Shock and Vibration, 2018.

- [6]. *Y. J. Cha, O. Buyukozturk*, “Structural damage detection using modal strain energy and hybrid multiobjective optimization”, in Computer-Aided Civil and Infrastructure Engineering, Vol, 30, no. 5, 2015, pp. 347-358.
- [7]. *G. Box, K. B. Wilson*, “On the experimental attainment of optimum conditions”, in Journal of the Royal Statistical Society Series B (Methodological), Vol. 13, no. 1, 1951, pp. 1-38.
- [8]. *S. Umar, N. Bakhary, A. R. Z. Abidin*, “Response surface methodology for damage detection using frequency and mode shape”, in Measurement, Vol. 115, 2018, pp. 258-268.
- [9]. *T. Mukhopadhyay, T. K. Dey, R. Chowdhury, A. Chakrabarti*, “Structural damage identification using response surface-based multi-objective optimization: a comparative study”, in Arabian Journal for Science and Engineering, Vol. 40, no. 4, 2015, pp. 1027-1044.
- [10]. *S. Rucevskis, M. Wesolowski*, “Identification of damage in a beam structure by using mode shape curvature squares”, in Shock and Vibration, Vol. 17, no. 4-5, 2010, pp. 601-610.
- [11]. *B. Deniz, H. Boyaci*, “Modeling and optimization I: Usability of response surface methodology”, in Journal of food engineering, Vol. 78, no. 3, 2007, pp. 836-845.
- [12]. Design Expert, User's Manual Version 8.0, 2007.
- [13]. *L. D. Goh, N. Bakhary, A. A. Rahman, B. H. Ahmad*, “Application of neural network for prediction of unmeasured mode shape in damage detection”, in Advances in Structural Engineering, Vol. 16, no. 1, 2013, pp. 99-113.
- [14]. *H. B. Xu, G. H. Chen*, “An intelligent fault identification method of rolling bearings based on LSSVM optimized by improved PSO”, in Mechanical systems and signal processing, Vol. 35, no. 1-2, 2013, pp. 167-175.